

Introduction

Observations of the time-variable Earth's gravity field describe the redistribution of environmental masses in the Earth system, including changes in land hydrology, ice, ocean, and atmosphere. These observations provide essential insights into the global water cycle, changes in ocean surface currents, mountain, and polar ice mass loss, large-scale underground droughts, sea-level rise, surface load displacements, as well as many other environmental processes. The variations of the Earth's gravity field directly influence the Earth's rotation, in particular, pole coordinates and length of the day variations from intra-annual to decadal and secular scales. The primary goal of this study is to analyze monthly temporary models from different solutions: from the GRACE mission and from SLR. We show trends and amplitudes in equivalent water high (EWH) in global and specific regions with prominent changes. Finally, we analyze the time series of selected zonal, tesseral, and sectorial spherical harmonics of significant interest and highlight the Empirical Orthogonal Functions (EOFs) for SLR solutions.

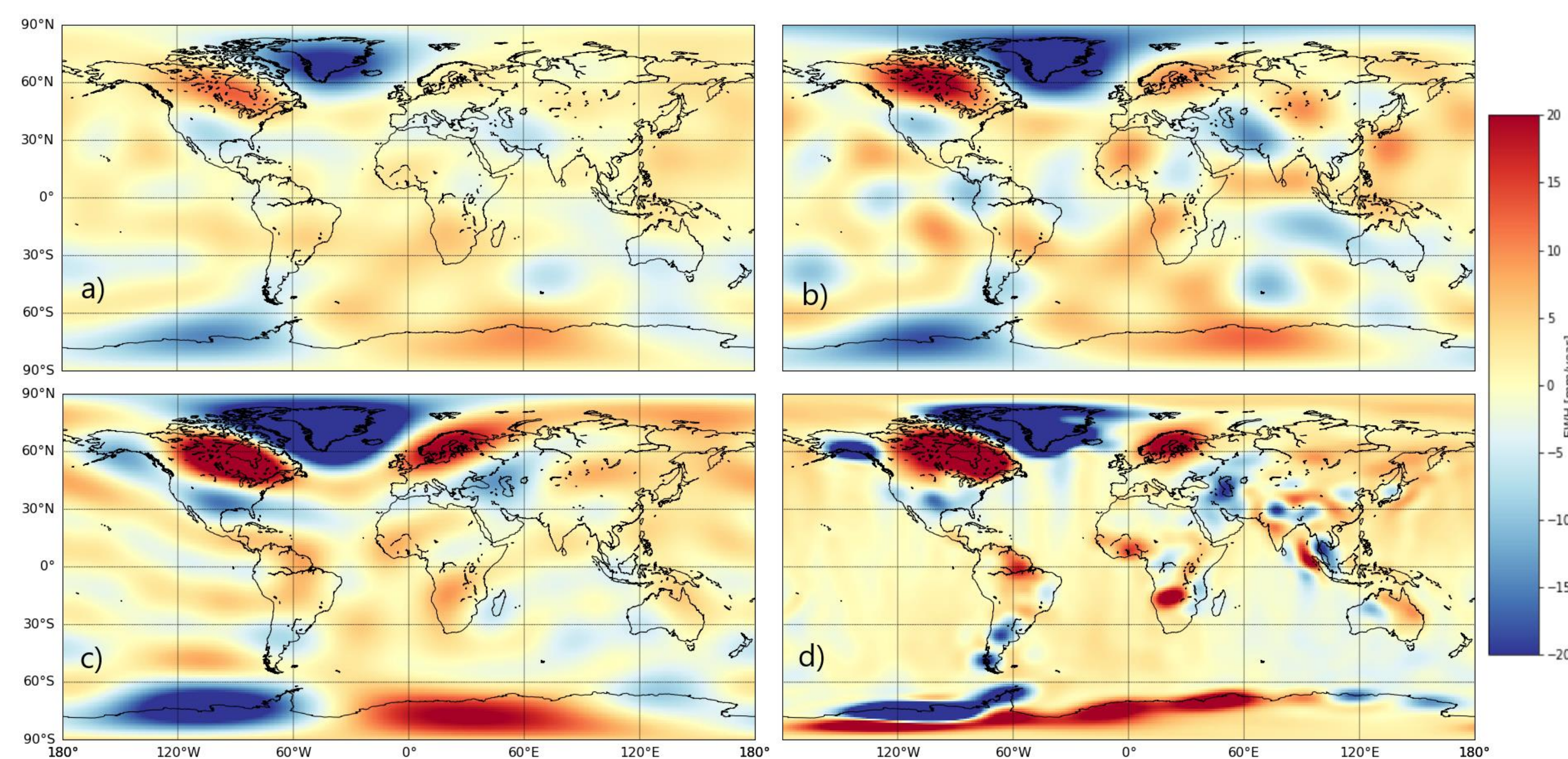


Fig 1. Global trend maps in terms of equivalent water height (EWH), a) – SLR constrained solution up to d/o 10/10, b) – SLR 10/10 new unconstrained solution with even-degree separation, c) – truncated JPL RL06 10/10, d) JPL RL06 60/60 + DDK3 + GAUSS 300km. The solutions a) and b) cover the period 1995.1 – 2014.6, c) and d) cover the period 2002.4 – 2014.6

SLR solution

Using SLR observations, we generate new Earth's gravity field coefficients. We use nine satellites, two of which are high orbiting LAGEOS, while the other seven are low-orbiting geodetic satellites such as LARES, Larets, Stella, AJISAI, BLITS, Starlette and Beacon-C. The gravity field is expanded up to degree and order (d/o) 10 with a monthly resolution for 1995.6–2014.6 with a simultaneous estimation of satellite orbits, Earth rotation parameters, and station coordinates. The solution from **Fig.1 a)** is a constrained solution up to d/o 10/10 as proposed by Sośnica et al. (2015). The solution from **Fig.1 b)** is based on the same normal equations, however, the solution was split into solutions expanded up to d/o 4/4, 6/6, 8/8, and 10/10 and stacked taking a benefit from the stability of low-degree expansion and a better resolution of high-degree solution expansion. The SLR results are compared with the Earth's gravity field from GRACE data (JPL RL06) truncated to d/o 10/10 and primary d/o 60/60 with two filters.

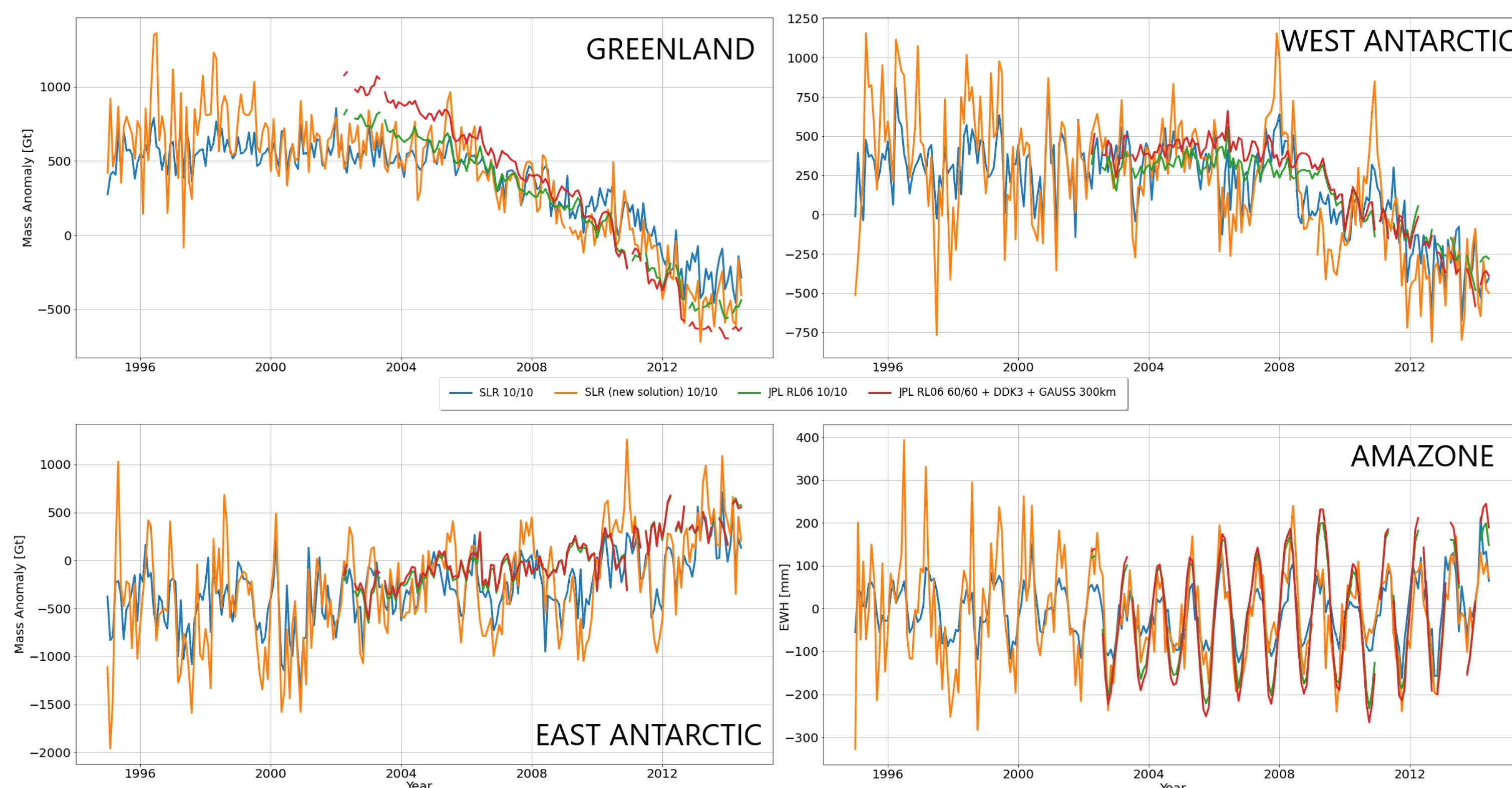


Fig 2. Time series of mass variations over the Greenland (top-left), West Antarctic (top-right), East Antarctic (bottom-left) and Amazon (bottom-right) derived from SLR (d/o 10/10) and GRACE JPL RL06 solutions, with coefficients truncated to d/o 10/10 and GRACE JPL RL06 nominal d/o 60/60, respectively.

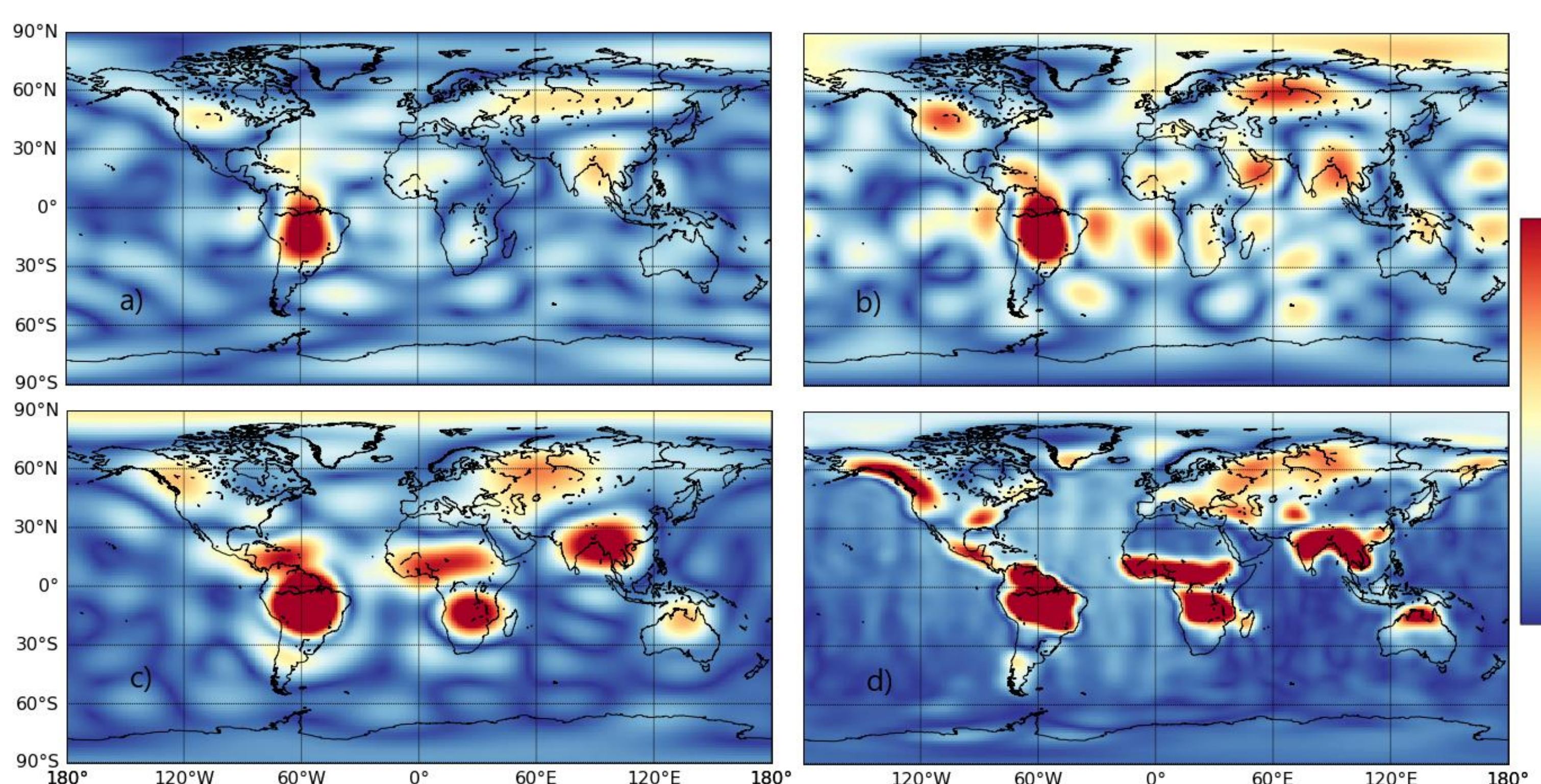


Fig 3. The overall EWH amplitudes of the annual signal from a) – SLR constrained solution up to d/o 10/10, b) – SLR 10/10 new unconstrained solution with even-degree separation, c) – truncated JPL RL06 10/10, d) JPL RL06 60/60 + DDK3 + GAUSS 300 km. The solutions cover the period 2002.4 – 2014.6

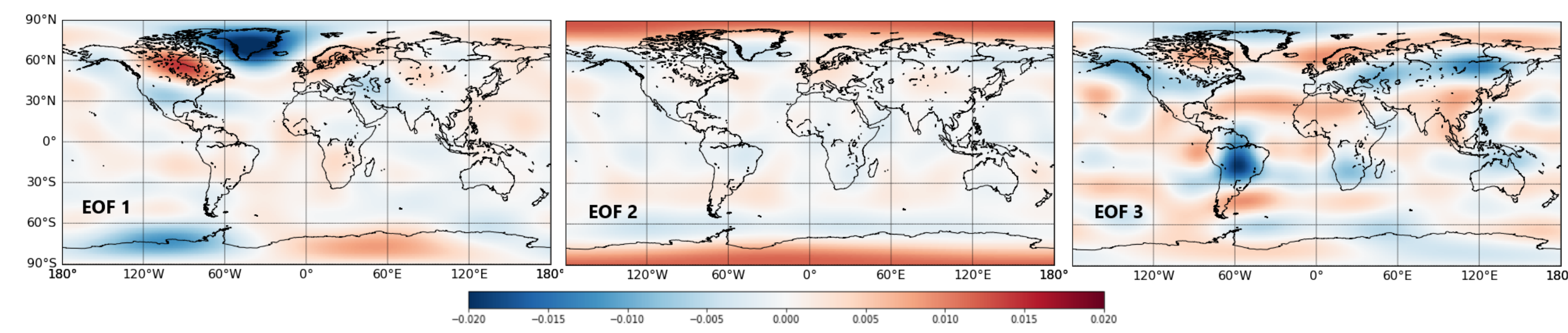


Fig 4. Empirical orthogonal functions from SLR (d/o 10/10) (1995.1 – 2014.6)

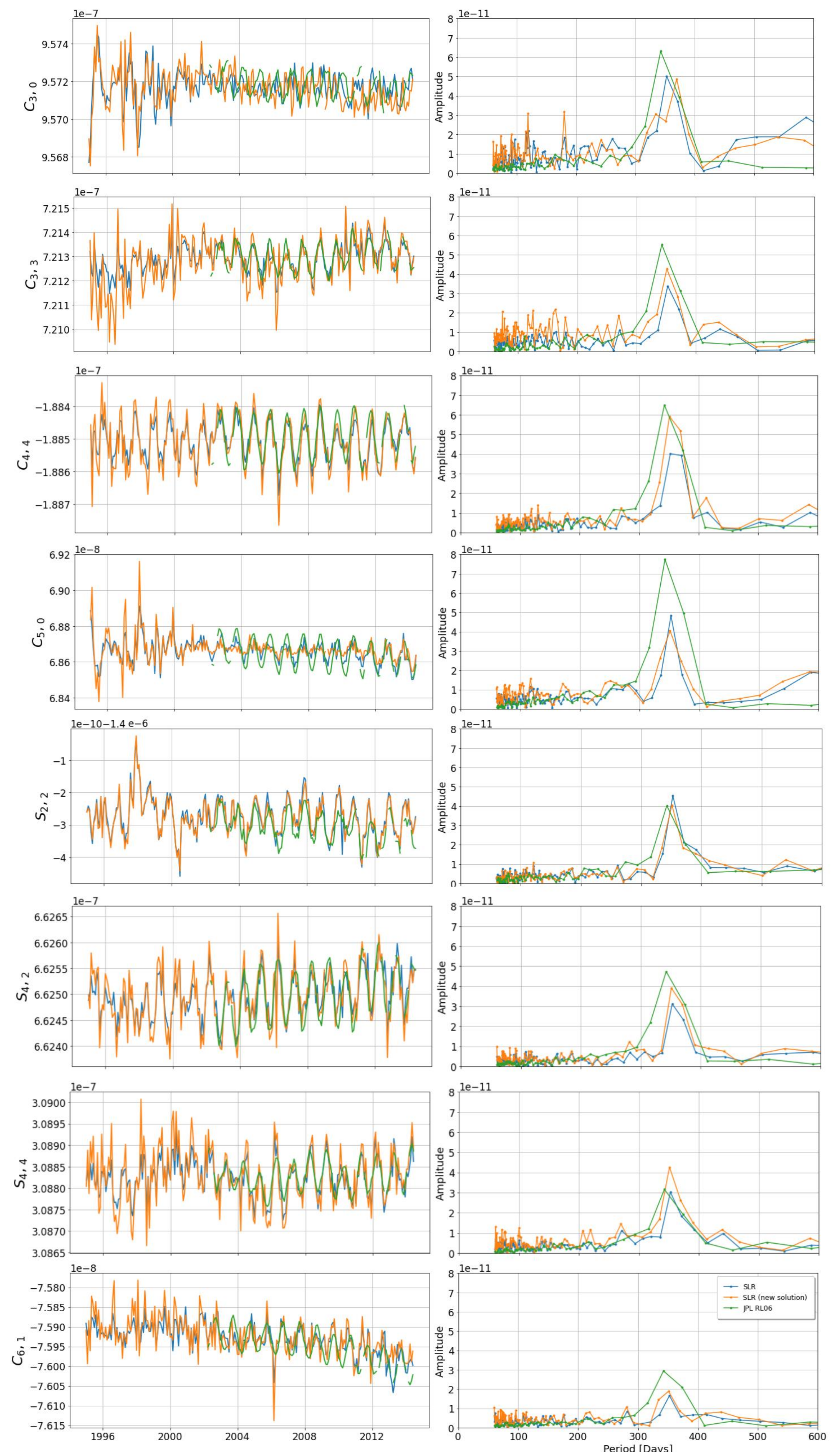


Fig 5. The spherical harmonics based on SLR-only up to d/o 10/10 constrained solution – blue, SLR-only up to 10/10 unconstrained (new solution) – orange, GRACE JPL RL06 – green.

Conclusion

The mean global trends in terms of EWH derived from GRACE and SLR are shown in **Fig. 1**. Global changes in trends in specific regions in all solutions are visible. When comparing SLR solutions in their new version, the areas related to glacial isostatic adjustment (GIA) like Scandinavia and North-East Canada are more visible. The climate change impact on ice field melting in Patagonia, western Antarctica, and Greenland are much more pronounced. The problems of water changes in the areas around the Aral Sea and the Caspian Sea are much more marked. Analyzing **Fig. 2**, we can see exactly in which year EWHs are accelerating, and in which they remain stable. In the case of Greenland and Antarctica, we can see their significant acceleration around 2003. SLR solutions also show a very high dependence in terms of amplitudes relative to GRACE solutions. There is also a lot of instability before 2000 due to fewer satellites observed by stations and poorer quality of observations before that time due to their worldwide distribution. In the case of the analysis of spherical harmonics in **Fig. 5** showing changes in the annual cycle, a high dependence between GRACE-derived solutions and SLR solutions is observed. This is the case with spherical harmonics $C_{3,3}$, $C_{4,4}$, $S_{2,2}$ and $S_{4,4}$. This relationship can also be seen in **Fig. 3**. In the case of the $C_{3,0}$ factor, a semiannual cycle is also visible. **Fig. 5** also reveals the period about 120 days. It can be related to Stella's revolution period of the perigee (122 days) or a peak related to Starlette's secular drift of the ascending node 121 days but these peaks are smaller than annual signals. **Fig. 4** shows the first three EOFs with non-randomness of the signal acquired from the SLR observations; the areas from the EOF decomposition coincide with the changes occurring in the redistribution of environmental masses in the Earth system. Finally, we see huge potential in using the SLR observations when recovering the time-variable gravity field especially when determining low-degree spherical harmonics.

This contribution was made as part of a project that is funded by the Polish National Science Centre (NCN 2021/42/E/ST10/00020)